Structure and membrane organization of photosystem II in green plants

Hankamer, B; Barber, J; Boekema, EJ

Published in:
Annual Review of Plant Physiology and Plant Molecular Biology

DOI:
10.1146/annurev.arplant.48.1.641

Publication date:
1997

Annu. Rev. Plant Physiol. Plant Mol. Biol. 1997. 48:641–71

STRUCTURE AND MEMBRANE ORGANIZATION OF PHOTOSYSTEM II IN GREEN PLANTS

Ben Hankamer and James Barber

Wolfson Laboratories, Department of Biochemistry, Imperial College of Science, Technology and Medicine, London SW7 2AY, United Kingdom

Egbert J. Boekema

Biophysical Chemistry, Groningen Biomolecular Sciences and Biotechnology Institute, University of Groningen, Nijenborgh 4, NL-9747 AG Groningen, The Netherlands

KEY WORDS: light harvesting, photosynthesis, photosystem II, structure, thylakoid membrane

ABSTRACT

Photosystem II (PSII) is the pigment protein complex embedded in the thylakoid membrane of higher plants, algae, and cyanobacteria that uses solar energy to drive the photosynthetic water-splitting reaction. This chapter reviews the primary, secondary, tertiary, and quaternary structures of PSII as well as the function of its constituent subunits. The understanding of in vivo organization of PSII is based in part on freeze-etched and freeze-fracture images of thylakoid membranes. These images show a resolution of about 40–50 Å and so provide information mainly on the localization, heterogeneity, dimensions, and shapes of membrane-embedded PSII complexes. Higher resolution of about 15–40 Å has been obtained from single particle images of isolated PSII complexes of defined and differing subunit composition and from electron crystallography of 2-D crystals. Observations are discussed in terms of the oligomeric state and subunit organization of PSII and its antenna components.

CONTENTS

INTRODUCTION 642
THE PHOTOSYSTEM II SUBUNITS: STRUCTURE AND FUNCTION 643
ARRANGEMENT OF PSII IN THE THYLAKOID MEMBRANE 648
Localization of PSII and LHCII 649

1040-2519/97/0601-0641$08.00

Heterogeneity of PSII In Vivo 649
STRUCTURE DETERMINATION BY ELECTRON MICROSCOPY 652
Single Particle Image Averaging 652
Electron Crystallography 655
SUBUNIT ORGANIZATION OF PSII 659
Localization of D1-D2-Cyt b559-CP47 Complex and CP43 659
Localization of the 33-kDa Extrinsic Subunits 659
Localization of the 23-kDa Extrinsic Subunits 662
Organization of the Membrane-Embedded PSII Core Components 662
Localization of the Lhcb Proteins 664
CONCLUDING REMARKS 665

INTRODUCTION[1]

Photosystem II (PSII) is a multisubunit complex embedded in the thylakoid membranes of higher plants, algae, and cyanobacteria. It uses light energy to catalyze a series of electron transfer reactions resulting in the splitting of water into molecular oxygen, protons, and electrons. These reactions occur on an enormous scale and are responsible for the production of atmospheric oxygen and indirectly for almost all the biomass on the planet. Despite its importance, the catalytic properties of PSII have never been reproduced artificially. Understanding PSII's unique chemistry is important and could have implications for agriculture as PSII is a main site of damage during environmental stress.

The chapter reviews our current knowledge of the three-dimensional structure of PSII in higher plants, an area of research that has developed rapidly over recent years. We first outline the photochemical reactions in this photosystem and summarize in a table the main structural features of individual subunits, focusing on their likely transmembrane helical content and cofactor binding properties. Electron microscopy of PSII is then reviewed to relate the subunit and cofactor composition of PSII to its three-dimensional structure. Low-resolution structural data on PSII, obtained from freeze-etch and freeze-fracture studies of thylakoid membranes, is reviewed initially. Such studies have provided information on the location, heterogeneity, and overall size and shape of PSII and its antenna system in the thylakoid membrane at resolutions of 40–50 Å. To obtain higher-resolution information (~15–40 Å), two other approaches have been used: single particle image averaging of detergent-solubilized PSII complexes and analysis of two-dimensional crystals. The former

[1] Abbreviations: β-Car, β-carotene; BChl, bacteriochlorophyll; Chl, chlorophyll; CD, circular dichroism; CP, chlorophyll protein; cyt *b*559, cytochrome *b*559; LHCII, light-harvesting complex of PSII; LH2, light-harvesting complex of purple photosynthetic bacteria; PSI, photosystem one; PSII, photosystem two; P680, primary electron donor of PSII; Pheo, pheophytin; PQ, plastoquinone; Q_A and Q_B, primary and secondary electron acceptors of PSII; RC, reaction center; STEM, scanning transmission electron microscopy

has yielded considerable information on the oligomeric state and subunit organization of PSII and its antenna system, whereas the latter offers the potential of a structure at atomic resolution. Results obtained from both approaches are discussed in terms of the question of whether PSII exists as a monomer or dimer in vivo. Finally, the conclusions emerging from these studies are compared with biochemical and cross-linking data.

THE PHOTOSYSTEM II SUBUNITS: STRUCTURE AND FUNCTION

Well over 20 subunits (PsbA–PsbX, Lhcb1–6) are associated with PSII of higher plants and green algae (Figure 1) and have been named after the genes

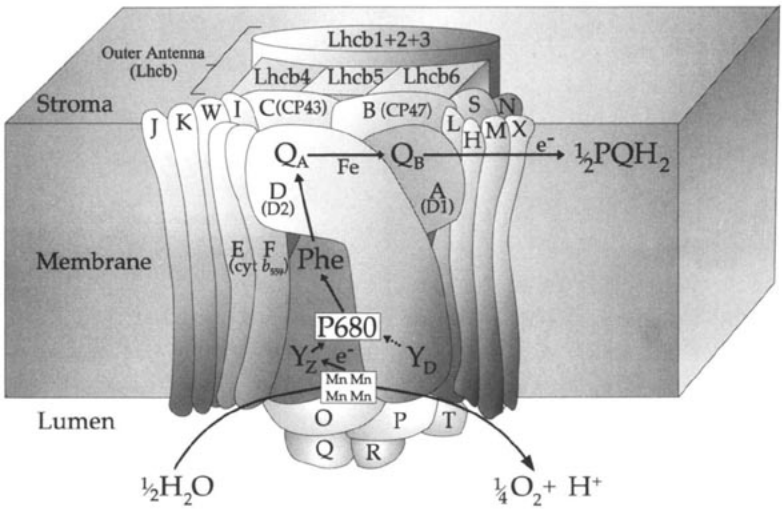

Figure 1 Photosystem II: an overview of subunit composition and electron transport. The PSII complex and its antenna system consists of more than 20 subunits that are either embedded in the thylakoid membrane or associated with its lumenal surface. Light energy is trapped predominantly in the outer antenna, consisting of the proteins Lhcb1–6. The excitation energy is transferred to the photochemically active reaction center (D1 and D2 proteins) via CP47 and CP43, where it is used to drive the water-splitting reaction. The electrons extracted from water are passed from the lumenally located four-atom Mn cluster to D1-Tyr 161 (Y_Z), $P680^+$, Phe, Q_A and on to Q_B, via a nonheme iron group. This electron transport pathway is marked with arrows. The protons and molecular oxygen produced during the water-splitting reaction are released into the lumen. The plastoquinone (PQ) bound at the Q_B site accepts two electrons derived from water via the electron transport chain and two protons from the stroma before being released into the thylakoid membrane in the form of PQH_2. The letter notation used for the subunits of the core complex reflects gene origin (e.g. A = product of *psbA* gene).

Table 1 The PSII subunits: primary and secondary structure, cofactor content, and function[a]

Gene	Subunit	Mass (kDa)	No. of transmembrane α-helices	Function
psbA	D1	38.021(S)	5	YZ & binds P680, Pheo, Q_B
psbD	D2	39.418(S)	5	YD & binds P680, Q_A
psbE	α-cyt b559	9.255(S)	1	Binds heme, photoprotection
psbF	β-cyt b559	4.409(S)	1	Binds heme, photoprotection
psbI	I protein	4.195(S)	1	?
psbB	CP47	56.278(S)	6	Excitation energy transfer, binds 33 kDa
psbC	CP43	50.066(S)	6	Excitation energy transfer, binds 33 kDa
psbH	H protein	7.697(S)	1	Photoprotection
psbK	K protein	4.283(S)	1	PSII assembly, PSII stability
psbL	L protein	4.366(S)	1	Involved in Q_A function
psbM	M protein	3.755(P)	1	?
psbN	N protein	4.722(T)	1	?
psbO	33-kDa ext. protein	26.539(S)	0	Stabilizes Mn cluster, Ca^{2+} & Cl^- binding
psbP	23-kDa ext. protein	20.210(S)	0	Ca^{2+} and Cl^- binding
psbQ	16-kDa ext. protein	16.523(S)	0	Ca^{2+} and Cl^- binding
psbR	R protein	10.236(S)	0	Donor and acceptor side functions
psbS	S protein	21.705(S)	4	Chl chaperonin/antenna component
psbT	T protein	3.283(S)	0	?
psbV	V protein*	15.121(Sy)	0	Donor side stability
psbW	W protein	5.928(S)	1	?
psbX	X protein	4.225(S)	1	Q_A function
lhcb4	Lhcb4 (CP29)	29	3	Excitation energy transfer & dissipation
lhcb5	Lhcb5 (CP26)	26	3	Excitation energy transfer & dissipation
lhcb6	Lhcb6 (CP24)	24	3	Excitation energy transfer & dissipation
psbJ	J protein	4.116(P)	1	PSII assembly
psbU	U protein*	10(Cy)	?	?
lhcb1	Lhcb1	25	3	Light harvesting
lhcb2	Lhcb2	25	3	Light harvesting
lhcb3	Lhcb3	25	3	Light harvesting

[a]Twenty-three putative PSII proteins are encoded by the *psbA–psbX* genes, whereas at least six outer antenna components are encoded by *Lhcb1–L–6*. The subunits encoded by these genes are listed according to the complexes with which they copurify (e.g. reaction centers), and those marked (*) have only been detected in cyanobacteria. The molecular masses of the mature PsbA–PsbX proteins, except PsbU, are calculated from the protein sequences reported in the SWISSPROT data base using the MacBioSpec program (Sciex Corp., Thornhill, Ontario, Canada). The abbreviations given in brackets after the molecular masses denote the organism for which the subunit mass is given, as

Chla	Chlb	β-Car	Pheo	Lut	Neo	Viol	
6	0	2	2	0	0	0	**PSII reaction center**
10–25	0	3	0	?	0	0	
9–25	0	5	0	?	0	0	
—	—	—	—	—	—	—	
—	—	—	—	—	—	—	
—	—	—	—	—	—	—	**Full PSII core**
—	—	—	—	—	—	—	
—	—	—	—	—	—	—	
0	0	0	0	0	0	0	
0	0	0	0	0	0	0	
0	0	0	0	0	0	0	
—	—	—	—	—	—	—	
5?	—	—	—	—	—	—	
—	—	—	—	—	—	—	
—	—	—	—	—	—	—	
—	—	—	—	—	—	—	
—	—	—	—	—	—	—	
9–10	3–4	—	0	1–2	1	1–2	**PSII core & minor CAB proteins**
7–9	4–5	—	0	2	0.5–1	0.5–1	
6	7	—	—	2	1	1	
—	—	—	—	—	—	—	
—	—	—	—	—	—	—	
8	6	0	0	2	0.5–1	0.5	**Full PSII & antenna complex**
8	6	0	0	2	0.5–1	0.5	
8	6	—	—	—	—	—	

follows: S, spinach; Sy, *Synechococcus* sp.; P, pea; T, tobacco. For the Lhcb proteins and PsbU, only the apparent molecular masses are provided. The next column lists the number of predicted transmembrane helices of each subunit. The putative functions of each subunit are given in the next column. The cofactors associated with the individual subunits are also listed as follows: Chla, chlorophyll a; Chlb, chlorophyll b; β-Car, β-carotene; Pheo, Pheophytin; Lut, lutein; Neo, neoxanthin; Viol, violoxanthin. The references reporting the information summarized in this table are given in the text.

encoding them (38, 46–49, 58, 65). The structure (22, 28, 33, 53, 65, 69, 79, 89, 97, 105, 111, 123, 129), cofactor organization (16, 22, 25, 38, 46–49, 53, 65, 69, 79, 89, 97, 108, 111, 123, 129), and function (32, 38, 46–49, 53, 62, 65, 69, 89, 97, 111) of these subunits have been studied in detail and are summarized in Table 1.

Figure 1 shows the subunit composition of PSII and its antenna system and indicates the photochemical processes that this photosystem catalyzes. The overall reaction driven by PSII is given in Equation 1, and all the cofactors involved are either bound within the reaction center proteins D1 and D2 or are closely associated with them.

$$2H_2O + 2PQ \xrightarrow[\text{PSII}]{\text{LIGHT}} O_2 + 2PQH_2 \qquad 1.$$

The light energy used to drive the water-plastoquinone (PQ) oxidoreductase reactions is captured predominantly by many molecules of chlorophyll (Chl) a and b [averaging about 250 per reaction center (70)] and carotenoid [β-carotene, lutein, neoxanthin, and violoxanthin (20, 69)] associated with light-harvesting antenna proteins, Lhcb1–6 (18, 21, 26, 46–49, 52, 65, 69, 97). The derived excitation energy is passed from the Lhcb proteins along an excitonically linked network of Chl molecules associated with CP47 (PsbB) and CP43 (PsbC) (18, 21, 22, 26, 65, 99, 100) to the PSII reaction center (RC). The RC consists of the D1 (PsbA) and D2 (PsbD) proteins (17, 91, 126), which are highly conserved between higher plant species and have a significant degree of local homology with the primary sequence of the L and M subunits of purple bacteria (16, 78, 110, 129). Ultimately the excitation energy derived from light is used to convert the primary oxidant, P680, to $P680^+$ (17, 91, 110, 111, 126). P680 is thought to consist of two Chl molecules ligated to the D1 and D2 proteins, though the excitonic coupling is much weaker than in the "special pair" of the purple bacterial reaction center (36, 111, 132). The excited state, P680*, donates a single high-energy unpaired electron to a molecule of pheophytin (Pheo), thereby forming the radical pair, $P680^+Pheo^-$ (17, 91, 126, 110, 111) (Figure 1). Each time $P680^+$ is formed, it accepts an electron from a specific amino acid residue (D1-Tyr161) and therefore is reduced to P680 (13, 25, 60, 98, 127). Illumination of PSII allows the P680, P680*, $P680^+$ cycle to be repeated and enables the sequential extraction of electrons from D1-Tyr161 (Figure 1). As D1-Tyr161 donates an electron to $P680^+$, it accepts another from water via a four-atom manganese (Mn) cluster, associated with the lumenal surface of PSII. Joliot et al (66) and Kok et al (68) used short light flashes to induce single turnovers of P680 and showed that the Mn cluster passed through a series of oxidation states referred to as the S_0-S_4 cycle. The

electrons, which are accepted by $P680^+$, are passed along the electron transport chain (Figure 1). In this way, Pheo accepts electrons from P680 and passes them on to a plastoquinone molecule (Q_A), tightly bound to the D2 protein (34, 71, 78, 107, 129). Q_A^- passes its electron on to a second plastoquinone molecule, associated with the Q_B site on the D1 protein (35, 59, 71, 78, 79, 96, 103, 105, 113). This electron transfer is aided by the presence of a nonheme iron located between Q_A and Q_B (16, 34, 79, 110). Each plastoquinone associated with the Q_B site can accept two electrons derived from water and two protons from the stroma before being released into the lipid matrix in the form of reduced plastoquinone (PQH_2).

The lumenal surfaces of membrane embedded CP47, CP43, and reaction center proteins of higher plants and green algae are in close contact with a number of extrinsic proteins. These include the products of the *psbO* (33-kDa subunit), *psbP* (23-kDa subunit), and *psbQ* (16-kDa subunits) genes, which together form the oxygen-evolving complex (OEC). The OEC also includes the Mn cluster (9, 25, 44, 89) and the three extrinsic proteins are involved in the optimization of its function in water splitting. The 33-kDa subunit stabilizes the Mn cluster (89) while the 23-kDa subunit allows PSII to evolve oxygen under both Ca^{2+}- (43, 89) and Cl^--limiting conditions (86, 87). This has led to the suggestion that the 23-kDa subunit acts as a concentrator of these ions (89). The 16-kDa polypeptide aids PSII to evolve oxygen efficiently under severely Cl^--limiting (<3 mM) conditions (2).

Except for subunit PsbS, all other subunits associated with PSII (Figure 1, Table 1) have a mass under 10 kDa (38). The exact number of the small subunits associated with PSII in vivo is not known, primarily because some of these proteins stain poorly and/or are difficult to resolve even in high-resolution gels (73). The reader is referred to the detailed review by Erickson & Rochaix (38) and the SWISSPROT data base for further information on the low-molecular-weight subunits of PSII, because their properties and those of the other PSII subunits are only summarized here (Table 1). Table 1 lists the subunits, in a way that reflects the PSII particle type that they are associated with, the smallest being the isolated reaction center and the largest being PSII with its complete antenna. The cofactors bound by each subunit are given, together with subunit function, common name, and the number of α-helices that the subunit is predicted to contain.

We now relate the information on the subunit structure summarized in Table 1 to structural information available on PSII and its antenna system.

ARRANGEMENT OF PSII IN THE THYLAKOID MEMBRANE

Much of our understanding of the in vivo organization of PSII is based on freeze-etched and freeze-fracture images of thylakoid membranes. Such electron microscopy studies provide structural detail at a resolution of about 40–50 Å and have provided information on the localization, heterogeneity, dimensions, and shapes of PSII and its antenna system.

By thin sectioning of fixed chloroplasts, electron microscopy has revealed the overall architecture of the thylakoid membrane of higher plants. The thylakoid membrane consists of two main compartments, the grana and the stroma lamellae. The stroma membranes form unstacked (nonappressed) regions, whereas the grana membranes are mostly present as stacked (appressed) membranes. There is a marked heterogeneity in lateral distribution of the major complexes of this membrane. It is generally accepted that PSII, photosystem one (PSI), and ATP synthase are mainly laterally segregated, with PSI and ATP synthase excluded from the appressed grana membranes and PSII abundantly present in the stacked parts of the thylakoid membrane (10, 15). The total picture, however, is more complex, because there is also heterogeneity among both PSII and PSI in subunit composition and lateral distribution (3).

In freeze-etching studies, thylakoids are flash frozen before the evaporation of surface water under vacuum (typically at −100°C). This process exposes the membrane surface and so allows the visualization of extrinsic components in their near-to-native state. The organization of the membrane embedded parts of PSII and the antenna proteins have been studied using the freeze-fracture technique, which involves the cleavage of the lipid bilayer along its internal hydrophobic plane, before image analysis. The terminology (ESs, PSs, ESu, PSu) used by Staehelin (120, 121) has generally been adopted to describe the endoplasmic (E) and protoplasmic (P) surfaces (S) of stacked (s) and unstacked (u) freeze-etched thylakoid membranes. The corresponding freeze-fracture (F) planes are referred to as EFs, PFs, EFu, and PFu.

The ultrastructure of thylakoid membranes of barley (55, 80), spinach (85, 119, 120, 122), maize (84), lettuce (56), soybean (67), *Alocasia* (7), and pea (11, 101) have all been analyzed by freeze-etch and freeze-fracture electron microscopy and show marked similarities (see 80, 121). The protein complexes detected in these analyses were named according to the surfaces with which they were associated (e.g. ESs or PFu particles). They differed in size and shape, and the constituent components of many were identified by the analysis of mutant membranes. For example, the analysis of PSI-deficient mutant thylakoid membranes showed that this photosystem formed part of the

large PFu particles (117). Localization of complexes in the thylakoid membranes was further facilitated by antibody labeling (95).

Localization of PSII and LHCII

Comparative freeze-etch and freeze-fracture studies of wild-type and PSII-deficient mutants of tobacco showed that the thylakoid membranes of the latter were depleted of ESs and EFs particles (81). From these results, it was concluded that the ESs and EFs particles corresponded to the extrinsic and internal parts of PSII, respectively. Support for this conclusion came from parallel studies of PSII-deficient barley mutants (*xantha*-b12, *viridis*-c12, *viridis* e-64, and *viridis* zd69), which showed that their granal membranes were also greatly depleted of EFs particles (e.g. 115, 121). The antenna proteins were located using Lhcb protein–deficient mutants (e.g. barley mutants *xantha*-l35 and *viridis*-k23 and *chlorina* f2) and by comparing thylakoid membranes from light- and dark-grown plants, the latter being depleted in these antenna proteins (12, 83, 116, 118). These studies showed that membranes depleted of Lhcb proteins lacked the PFs particles found in wild-type membranes. Freeze-etch images of membranes depleted of Lhcb protein also showed the ESs particles to be smaller. Together, these results suggested that the PFs particles contained the antenna proteins and that they were closely associated with PSII (EFs and ESs) particles.

The close association of PSII and the Lhcb proteins was characterized in more detail by the analysis of 2-D crystalline arrays of ESs complexes. Images of such ordered arrays showing a section of their freeze-etch surface (ESs surface) and a part of the protoplasmic fracture face (PFs surface) were presented by Miller (80) and Simpson (116). They showed that the Lhcb proteins (PFs particles in the PFs fracture face) fitted in register into the grooves between the PSII complexes (ESs particles in the freeze-etched ESs surface).

Heterogeneity of PSII In Vivo

The ESs and EFs particles that contain PSII are not evenly distributed within the thylakoid membrane. Freeze-etch and freeze-fracture studies have shown that ESs and EFs particles, respectively, can be organized into 2-D arrays or be more randomly dispersed within the grana. PSII-like particles are also observed in the stroma lamellae. It has been calculated that 85% of PSII particles are located in the granal stacks. They are called PSIIα. The remaining 15% of PSII complexes are located in the stroma and are called PSIIβ (3, 10). PSIIα complexes have approximately twice the antenna size of the PSIIβ complexes (8) and are more efficient at reducing ferricyanide and duroquinone (57).

Because PSIIα complexes are more abundant and active than PSIIβ and because all the available structural data on PSII have been collected from such types of complexes, we focus on them in the sections below.

The PSIIα population in the grana can itself be divided into subpopulations of differing antenna size (4, 5). Interestingly, freeze-etch studies have shown that some ESs particles within the grana form 2-D arrays, whereas others are more randomly dispersed and so form at least two subpopulations (112, 116).

Several publications provide the dimensions of arrayed ESs particles. Wild-type ESs arrays in barley have unit cell dimensions of 175 × 247, 180 × 225, and 180 × 240 Å (82, 115). ESs arrays in spinach had an almost rectangular lattice with spacings of 175 × 204 Å (112), while those in the grana of two fatty acid desaturase mutants of *Arabidopsis thaliana* had unit cell dimensions of 190 × 230 Å and 180 × 230 Å (131). Closer analysis of the arrayed ESs particles showed them to have a tetramer-like appearance on their lumenal (ESs) surface and a height of 82 Å perpendicular to the membrane plane (112, 116). Sequential removal of the 16, 23, and 33 kDa proteins of the OEC resulted in a height reduction to 78, 74, and 61 Å, respectively (112). The removal of all three polypeptides exposed the membrane-embedded portion of the PSII-LHCII supercomplex and revealed it to have a dimer-like structure. This led to the conclusion that the ESs particle is a dimeric PSII-LHCII supercomplex and that the tetramer-like appearance of its lumenal surface reflects the organization of two copies of the OEC. Dimeric PSII-LHCII supercomplexes (Figure 2*D*) isolated by solubilization in detergent have been biochemically and structurally characterized (21, 52, 93). The structure of the isolated complex can be computationally aligned to form an array with a spacing of 190 × 210 Å and a similar lumenal surface topology to ESs particles (21, 52, 112). It is therefore possible that ESs-type arrays consist of dimeric PSII-LHCII supercomplexes of the type reported by Boekema et al (21).

One argument that could be raised against the proposal that the ESs particles consist of dimeric PSII-LHCII supercomplexes of this type is that, on average, PSII reaction centers in the grana are associated with about 250 Chl molecules (70). Thus a dimeric complex of PSII would be expected to bind about 500 Chl as opposed to the 200 Chl per RC found for the isolated PSII-LHCII supercomplex (21, 93). There is insufficient space within the unit cell of the constructed ESs lattice to accommodate the extra Lhcb subunits that would be required to bind an additional 300 Chl molecules. However, it should be stressed that the value of 250 Chl:RC obtained for granal membranes is an average value and that the randomly organized ESs particles within the grana are spaced sufficiently widely to allow them to be associated with much larger antenna systems (>250 Chl:RC). This hypothesis fits both the finding that the

Annu. Rev. Plant. Physiol. Plant. Mol. Biol. 1997.48:641-671. Downloaded from arjournals.annualreviews.org
by University of Groningen on 11/17/06. For personal use only.

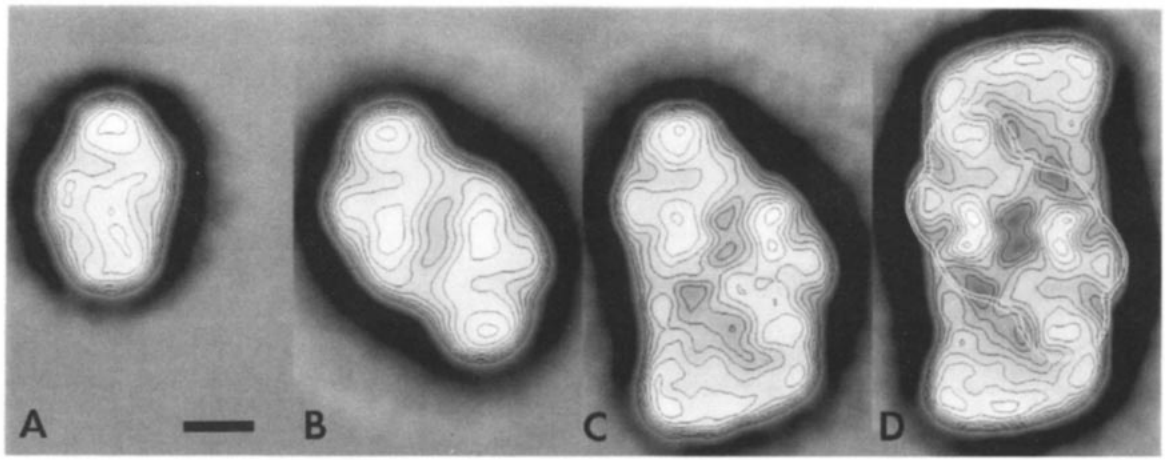

Figure 2 Top view projection maps of spinach PSII complexes obtained from nonperiodic (single particle) averaging of electron microscopy images obtained after negative staining. (*A*) A monomeric PSII core complex (240 kDa) consisting of CP47, CP43, the D1 and D2 proteins, cyt *b*559, the 33-kDa extrinsic protein, and associated low-molecular-weight polypeptides; (*B*) a dimeric PSII core complex (450 kDa) of the same subunit composition as the PSII core monomer; (*C*) a PSII-LHCII supercomplex consisting of a PSII core dimer and one set of Lhcb proteins (Lhcb1, 2, 4, and 5); (*D*) a PSII-LHCII supercomplex consisting of a PSII core dimer and two sets of Lhcb proteins (Lhcb1, 2, 4, and 5). The outline of the PSII core dimer shown in (*B*) is superimposed upon the PSII-LHCII supercomplex (*D*) to show the central location of the PSII core dimer. All the images are similar to those published by Boekema et al (21), but they differ in that they are the averages of larger data sets and so have an improved resolution (approximately 20 Å). Note: a twofold rotational symmetry has been imposed on images *B* and *D*. The scale bar measures 5 nm.

grana contain 250 Chl:RC on average and that the PSIIα population consists of subpopulations differing in antenna size (4, 5).

STRUCTURE DETERMINATION BY ELECTRON MICROSCOPY

X-ray crystallography is a powerful technique for elucidating the structure of proteins and has been particularly successful with photosynthetic membrane proteins. Atomic structures exist for the reaction center (6, 27–29) and the light-harvesting complex (LH2) (77) of photosynthetic purple bacteria. A map of near-atomic resolution also exists for PSI (42). Recently, the structure of the mitochondrial cytochrome *b-c* complex has been solved at atomic resolution, thus providing structural information relevant to the related photosynthetic cytochrome b_6f complex (137). Despite these striking successes, the X-ray approach has not revealed the structure of PSII. Adir et al (1) and Fotinou et al (40) have grown 3-D crystals of PSII cores, but they were too small and insufficiently ordered for high-resolution analyses.

In the absence of highly ordered 3-D crystals suitable for X-ray diffraction analyses, electron microscopy offers an alternative approach. Two techniques are available: single particle image averaging and electron crystallography using 2-D crystals. Both have been applied to elucidate the structure of PSII and in principle could yield maps at atomic resolution (54). To date, both techniques have yielded information on the oligomeric state (monomers vs dimers) of PSII in vivo and on its subunit organization.

Single Particle Image Averaging

Single particle analysis has been used to study the structure of a wide range of biological molecules, either imaged in negative stain or in vitreous ice (cryo-electron microscopy). Data obtained from biological molecules in vitreous ice correspond most clearly with the native protein structure and typically have a resolution up to 15 Å. Conventionally negatively stained samples (air dried and imaged at room temperature) usually give lower resolution (approximately 20 Å). The images obtained are classified according to the orientation of the particle (e.g. top and side views), and members of each class are then rotationally and translationally (i.e. shifted in the X-Y plane) aligned. The procedure is more useful for large particles (>250 kDa), which can be more accurately aligned.

The single particle image averaging approach has been used to analyze a number of detergent-solubilized PSII complexes of known subunit composi-

tion and oligomeric state (i.e. monomers and dimers) under negative stain conditions. The smallest higher plant PSII complex analyzed using this approach is a monomeric PSII core (approximately 240 kDa) consisting of CP47, CP43, D1, D2, cyt *b*559, the 33-kDa subunit, and associated low-molecular-weight polypeptides, together with about 36 Chla molecules (21, 51, 52). This complex is depicted in its top view orientation in Figure 2*A*. A dimeric complex of identical subunit composition and having an apparent molecular mass of 450 kDa is shown in its top view orientation in Figure 2*B*. By comparing Figures 2*A* and 2*B*, it can be seen that the projection map of the monomeric complex corresponds well with each half of the PSII core dimer. The dimensions of the latter were calculated to be 206 × 131 Å in the presence of the detergent (dodecyl maltoside) shell. When a detergent layer of 17 Å is deducted (30), the corrected dimensions of the isolated dimer are calculated to be 172 × 97 Å (21). Single particle analysis has also identified a PSII core dimer of similar size isolated from the cyanobacterium *Synechococcus elongatus* (21).

Although the dimeric organization of PSII has been readily accepted for cyanobacteria, there is currently a debate about whether the PSII particles in the grana are monomeric or dimeric complexes. It has been argued that dimeric PSII complexes, such as the one shown in Figure 2*B*, that were isolated from granal membranes, are the product of aggregation of PSII monomers rather than an in vivo form of PSII (39, 61, 92). A considerable volume of evidence speaks against this hypothesis. Freeze-etch images of thylakoid membranes showed that PSII complexes (ESs particles) located in the grana were most probably dimers (112). Holzenburg et al (61) argued that at the relatively low resolution of such freeze-etch images and of projection maps of crystallized dimer-like complexes (19), a pseudosymmetry relating to the similarity in structure of the D1 vs D2 proteins and CP47 vs CP43 proteins could be mistaken for a real twofold symmetry indicative of a dimeric complex. Consequently, it was suggested that PSII was actually a monomeric pseudosymmetric complex. To address this point, PSII complexes derived from gently solubilized granal and stromal membranes were analyzed under nondenaturing electrophoresis conditions. The granal PSII fraction consisted predominantly of dimeric PSII complexes associated with Lhcb proteins, while their stromal counterparts were monomeric (109). This result also showed that the nondenaturing electrophoresis conditions used did not induce aggregation of monomeric PSII (109). Other nondenaturing gel electrophoresis studies of this type came to the similar conclusion that PSII in the grana is dimeric (99). Furthermore, our own data (51, 52) has shown that isolated PSII core dimers (Figure 2*B*) were more active in terms of oxygen evolution, are associated with higher

levels of Chla (39 Chla:2 Pheo), and have much lower levels of D1 and D2 breakdown fragments than their monomeric counterparts (Figure 2*A*). Based on this information it is difficult to see how two damaged monomers could aggregate to form an intact dimer of the type shown in Figure 2*B* (51, 52). Taken together, these and other studies (see section on "Heterogeneity of PSII In Vivo") strongly suggest that PSII is a dimer in the grana.

Recently, grana membranes were solubilized with a single gentle solubilization step, to obtain a more native PSII complex. The solubilized mixture was then resolved by sucrose density gradient centrifugation. The largest PSII complex (approximately 700 kDa) consisted of the PSII core dimer subunits (Figure 2*B*) plus Lhcb1, 2, 4, and 5 proteins and contained about 200 Chl molecules (156 Chla, 4 Chlb) (21, 93). Like the PSII monomer (Figure 2*A*) and dimer (Figure 2*B*) cores, this PSII-LHCII supercomplex was active in oxygen evolution. Single particle analysis showed an unsymmetrized form of this PSII-LHCII supercomplex (Figure 2*D*) to have a clear twofold rotational symmetry axis around the center of the complex, consistent with a dimeric structure (21). Superimposed upon the projection map of the PSII-LHCII supercomplex (Figure 2*D*) is the outline of the PSII core dimer depicted in Figure 2*B*. This alignment of Figures 2*B* and 2*D* shows that the PSII core dimer forms the central part of the PSII-LHCII supercomplex (Figure 2*D*) and that the two regions flanking it must contain the Lhcb proteins. Figure 2*C* shows a PSII-LHCII complex from which one of the Lhcb protein sets has dissociated. This form of PSII-LHCII complex (Figure 2*C*) lacks the twofold symmetry of the PSII-LHCII supercomplex (Figure 2*D*) due to the loss of this single Lhcb set. Nevertheless the PSII core region is clearly twofold symmetric and closely resembles the averaged PSII core dimer top view (Figure 2*B*). Furthermore the structural features of the remaining Lhcb set (Figure 2*C*) correspond closely with that of the symmetric PSII-LHCII supercomplex. These findings confirm the true twofold symmetry and hence the dimeric nature of the PSII core.

After correction for the detergent layer, the PSII-LHCII supercomplex shown in Figure 2*D* is calculated to have dimensions of 270 × 125 Å. In its side view orientation, the particle has a thickness of about 60 Å in the Lhcb region, consistent with the height of LHCII (69, 133). Its maximal thickness, close to the center of the complex, is about 90 Å. This dimension is similar to that of the arrayed ESs particles observed in freeze-etch and freeze-fracture images of thylakoid membranes of a number of higher plant species (see section on "Heterogeneity of PSII In Vivo"). This suggests further that the ESs (EFs) particles are probably dimeric PSII-LHCII supercomplexes, as discussed above.

Electron Crystallography

The successful application of the other type of high-resolution electron microscopy (electron crystallography) in the determination of the atomic structure of trimeric LHCII demonstrates the power of this approach (69). Figure 3 shows that within each Lhcb protein monomer of LHCII, the two longest transmembrane helices are surrounded by Chla and Chlb molecules, and two molecules of lutein. The chlorophylls are arranged in two layers, toward the lumenal and stromal membrane surfaces, and the main ligands are Glu, Asn, Glu, His, and Gly. The close association of the luteins with the excitonically linked chlorophylls prevents singlet oxygen formation and the damage induced by it (69). The luteins also play a structural role in that they form a cross-brace in the center of the complex, providing a direct and strong link between the peptide

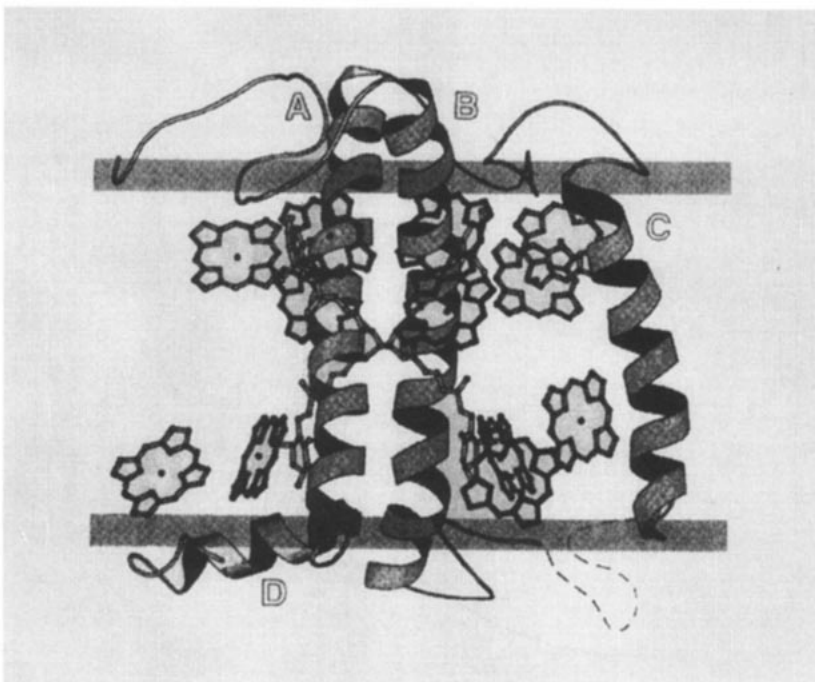

Figure 3 The structure of LHCII. This figure is taken from Kühlbrandt (69) and shows a folding model of a monomeric LHCII subunit. The LHCII monomer has three transmembrane α-helices (*A–C*) and a shorter helix (*D*) toward the lumenal surface of the membrane. The chlorophylls are arranged in two layers close to the stromal and lumenal surfaces of the membrane. Two Lut residues (L) form a cross-brace between helices A and B and are excitonically linked to the chlorophyll (Chl) network. Sequence homology between the subunits Lhcb1–6 suggests that all their structures will be similar.

loops at both surfaces (69). Based on the high degree of sequence homology, it is likely that the atomic structures of the other Lhcb proteins will also be similar to that of the LHCII monomer.

Isolated PSII complexes have also been crystallized when reconstituted with detergent solubilized lipid (31, 51, 90, 130). Another 2-D crystallization approach involves a detergent-induced delipidation step of granal membranes enriched in PSII and Lhcb proteins. This forces the complexes in the granal membranes into close contact and has yielded small 2-D crystals of PSII (19, 39, 61, 74–76, 109).

To compare the projection maps obtained using single particle image averaging (Figure 2) and electron crystallography (Figure 4), the isolated PSII core dimer shown in Figure 2*B* (51) was reconstituted with thylakoid lipid and crystallized, though the 33-kDa extrinsic protein dissociated during the process. The top view projection map, obtained from this D1-D2-cyt *b*559-CP47-CP43 complex, under negative stain conditions, is shown in Figure 4*A*. The first important point to note is that the unit cell of the crystallized PSII core dimer (a = 117 Å × b = 173 Å, $\gamma = 110°$) compares well with the size of the single particle averaged image of this complex (97 × 172 Å). The second is that the structural features of the two images are almost identical. The most prominent features are two densities (marked with * in Figure 4*A*), which are positioned on either side of a central hole. Although the projection map shown in Figure 4*A* is unsymmetrized, it clearly has a twofold rotational symmetry around its center, confirming its dimeric structure. Image sections taken through the 3-D image of this complex show it to have twofold symmetry throughout (E Morris, B Hankamer, D Zheleva & J Barber, unpublished data).

The top view projection map of another PSII crystal, imaged under cryo conditions, is shown in Figure 4*B*. The crystal was produced by delipidating granal membranes (75). A comparison of Figures 4*A* and 4*B* shows that the two projection maps have very similar features, including a central hole and two predominant regions of density, on either side of it (marked with a *). The two crystal forms also have very similar unit cell dimensions to that of the complex shown in Figure 4*B* (a = 114 Å, b = 173 Å, $\gamma = 106.6°$). Despite the similarity of the two projection maps and their unit cell dimensions, the crystals of Marr et al (75) were reported to contain Lhcb4, 5, and 6 and PsbS, in addition to the other PSII subunits of the complex shown in Figure 4*A*. Marr et al (75) came to this conclusion based on direct immunolabeling of their crystals. This apparent discrepancy remains to be resolved because the complex shown in Figure 4*A* does not contain these subunits.

Holzenburg et al (61) and Ford et al (39) also reported projection maps of crystallized PSII complexes with and without the extrinsic subunits of the

Annu. Rev. Plant. Physiol. Plant. Mol. Biol. 1997.48:641-671. Downloaded from arjournals.annualreviews.org
by University of Groningen on 11/17/06. For personal use only.

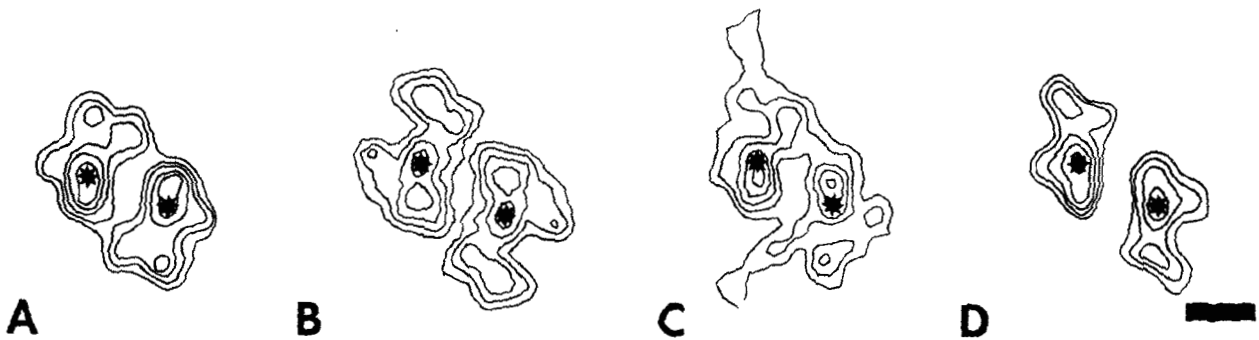

Figure 4 Projection structures of spinach PSII complexes obtained by crystallographic averaging of electron microscopy images of 2-D crystals. (*A*) A nonsymmetrized projection map of a crystallized PSII core dimer of the type shown in Figure 3*A*, consisting of CP47, CP43, the D1 and D2 proteins, cyt *b*559, and associated low-molecular-weight polypeptides but lacking the 33-kDa protein (E Morris, B Hankamer, D Zheleva & J Barber, unpublished results). (*B*) A filtered 2-D crystal projection map with twofold rotational symmetry imposed (redrawn from 75). (*C*) Nonsymmetrized section from the 3-D model of Ford et al (39), redrawn. (*D*) A nonsymmetrized filtered projection map of a 2-D crystal from Tsiotis et al (130), redrawn. In each of these four images, two prominent densities marked (*) are located in equivalent positions on either side of a central hole. The similarity in size and shape of these contoured maps suggests that all these complexes are dimeric. The scale bar measures 5 nm.

OEC. As in the case of Marr et al (75), these crystals were formed by partially delipidating granal membranes. To aid comparison with Figures 4*A* and 4*B*, the images of the crystal form lacking the extrinsic proteins are shown in Figure 4*C* (39). It is reported to have a unit cell (a = 177 Å, b = 201Å, $\gamma = 91°$) that is slightly larger than those of the dimeric PSII complexes shown in Figure 4*A* and 4*B*. On the basis of SDS-PAGE analysis, the authors concluded that their crystals contained both PSII core and Lhcb subunits. One of the difficulties in determining the subunit composition of a complex crystallized by the partial delipidation of granal membranes is to confirm the presence of given subunits in the crystalline fraction, when both crystalline and noncrystalline material is contained in the sample. Without direct immunolabeling of the crystals, their composition must remain unconfirmed. However, on the basis of the assumption that Lhcb proteins are associated with the crystallized complex, it was concluded that the PSII core complex must be monomeric because there was insufficient volume to accommodate a PSII core dimer and a large complement of Lhcb proteins (61). However, a comparison of the unsymmetrized images of Figures 4*A*, 4*B*, and 4*C* show them to be very similar. Once again, the same two prominent regions of density (*), also seen in Figures 4*A* and 4*B*, are apparent on either side of a central hole in Figure 4*C*. This suggests that this core complex may actually be a core dimer rather than a monomeric PSII complex and that its symmetry was mistaken as pseudosymmetry because of the relatively low resolution of the images.

Tsiotis et al (130) recently reported the projection maps of a PSII crystal (CP47, CP43, D1, D2, cyt *b*559, the 33-kDa extrinsic subunit, and associated low-molecular-weight polypeptides) obtained using detergent solubilized PSII core complexes (Figure 4*D*). This crystal was reported to have a unit cell of (a = 162 Å, b = 137Å, ($\gamma = 142.°$). However, if a choice of unit cell parameters is made to include all the densities shown in Figure 4*D*, the dimensions are actually very close to the ones reported by Hankamer et al (51) (Figure 4*A*) and Marr et al (75) (see Figure 4*B*). Furthermore, a central hole (or cavity) is visible in these complexes and two densities (*) are once again seen on either side of it, separated by about the same distance. All these points would suggest that this complex could also be a dimeric PSII core complex, although the authors concluded that the complex was a monomer, partly because of scanning transmission electron microscopy (STEM) measurements that suggested the complex had a mass of 318 kDa (130).

Recently, Nakazato et al (90) reported the crystallization of a D1-D2-cyt *b*559-CP47 complex, which yielded a projection map of 20-Å resolution. The projection map of this complex can be superimposed upon a PSII core monomer (Figure 3*A*) and comfortably fits into it (see Figure 5 and associated

discussion). This finding confirms that the PSII complexes depicted in Figures 4*A* and 4*B*, and probably in 4*C* and 4*D*, are dimeric.

SUBUNIT ORGANIZATION OF PSII

This section reviews the subunit organization of PSII and its antenna system using information that has been obtained by electron crystallography, single particle image averaging, and crosslinking and other biochemical techniques. The combined data is summarized in the form of two currently favored subunit organization models (Figures 5*a* and 5*b*) because the information available is still insufficient to confirm which of these is correct.

Top (Figures 5*a* and 5*b*) and side view (Figure 5*C*) projection maps of the largest PSII-LHCII supercomplex structurally characterized to date are used as the framework for the two possible models of subunit organization. These contoured projection maps are very similar to those presented by Boekema et al (21) but improved in that they are the sums of larger data sets (1925 vs 500 top views, 2213 vs 80 side views) and have a higher resolution (approximately 20 Å). They also differ in that they contain the densities of two 23-kDa subunits in addition to those of the other core (CP47, CP43, D1, D2, the 33-kDa subunit, cyt *b*559) and antenna (Lhcb1, 2, 4, and 5) (21, 93) proteins. Both models are identical in terms of their depiction of the extrinsic and Lhcb protein components. They differ only in the attributed locations of the PSII core components, CP47, D1, D2, and cyt *b*559.

Localization of D1-D2-Cyt b559-CP47 Complex and CP43

Regions within each of the projection maps are shaded in dark, mid, and light gray. The dark-gray regions represent aligned monomeric D1-D2-cyt *b*559-CP47 complexes (and associated low-molecular-weight subunits) of the type reported by Dekker et al (31) and Nakazato et al (90). Together, the two dark- and two mid-gray regions (Figures 5*a* and 5*b*) depict the shape of the PSII core dimer (Figure 2*b*) consisting of the integral membrane protein components D1, D2, cyt *b*559, CP47, and CP43 and associated low-molecular-weight subunits. By elimination, it follows that the two mid-gray regions each contain CP43 (106).

Localization of the 33-kDa Extrinsic Subunits

Top and side view projection maps of PSII complexes (±33-kDa extrinsic subunit) were used to produce subunit difference maps (21, 30). In Figure 5 each monomeric portion of the dimer is associated with a region of density attributed to the 33-kDa subunit, and these densities overlap to form a single

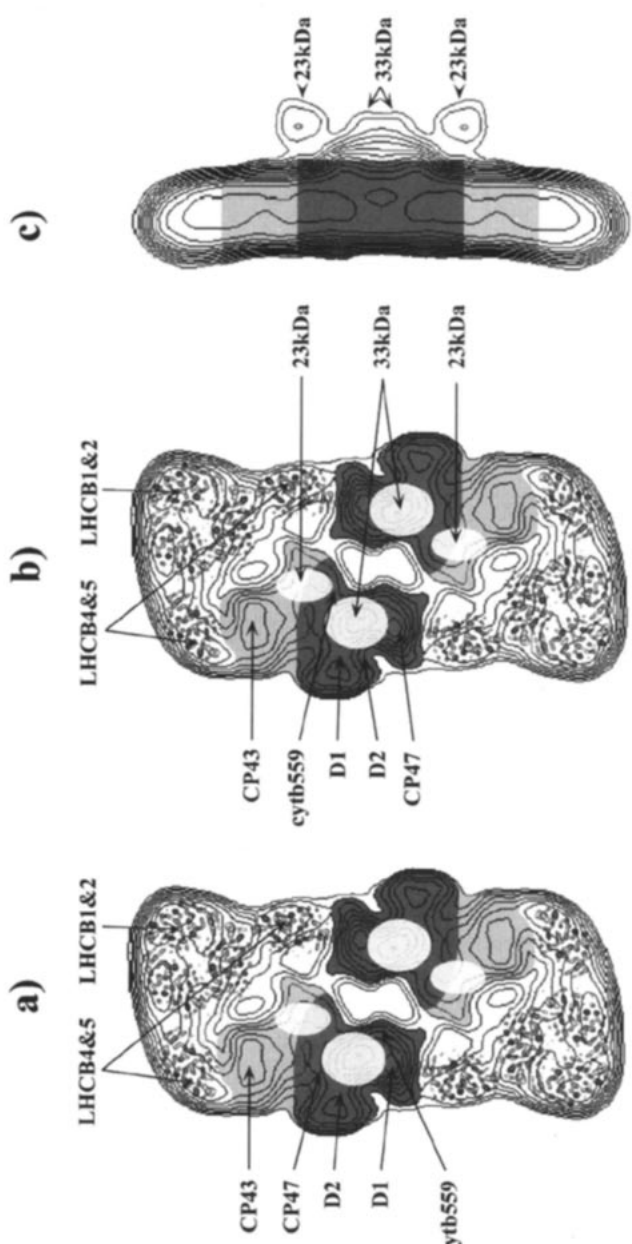

Annu. Rev. Plant. Physiol. Plant. Mol. Biol. 1997.48:641-671. Downloaded from arjournals.annualreviews.org
by University of Groningen on 11/17/06. For personal use only.

Figure 5 Subunit organization models of photosystem II. This figure shows top (Figures 5*a* and 5*b*) and side view (Figure 5*c*) projection maps of the largest PSII-LHCII supercomplex structurally characterized to date. It provides the framework for two possible models of subunit organization (Model 1 and Model 2), based predominantly on crosslinking studies and averaged images of PSII complexes of known and differing subunit composition. Both models are identical in terms of their depiction of the extrinsic and Lhcb protein components. They differ only in the attributed locations of the PSII core components, CP47, D1, D2, and cyt *b*559. In Model 1, CP47 is placed between CP43 and the reaction center components. In Model 2, the RC components are placed between CP47 and CP43. The three contoured projection maps (*a*, *b*, and *c*) are very similar to those presented in Boekema et al (21) but are improved in that they are the sums of larger data sets (1925 vs 500 top views, 2213 vs 80 side views) and have a higher resolution (approximately 20 Å). They also differ in that they contain the densities of two 23-kDa subunits in addition to those of the other core (CP47, CP43, D1, D2, the 33-kDa subunit, cyt *b*559) and the antenna (Lhcb1, Lhcb2, Lhcb4, and Lhcb5) (21, 93) proteins. Superimposed upon the central regions of each of these images are areas shaded in dark, mid, and light gray. Each of the two dark-gray regions corresponds to a monomeric CP47-RC complex similar to those reported by Dekker et al (31) and Nakazato et al (90). Together the two dark- and two mid-gray regions depict the centrally located CP47-CP43-RC core dimer (21). The four densities shaded in light gray in the top view projections (*a* and *b*) correspond to two 33-kDa and two 23-kDa subunits (21; see text). In the side view orientation (*c*) the two lumenally exposed 33-kDa subunits partially overlap. Positioned on either side of them are two densities attributed to the 23-kDa extrinsic proteins. The electron density map of an LHCII trimer (133) has been superimposed upon the two tips of the PSII-LHCII complex (*a* and *b*). It is suggested that these trimers consist of Lhcb1 and Lhcb2 and that they are linked to the centrally located PSII core via two monomeric Lhcb proteins (Lhcb4 and Lhcb5). The Lhcb4 and Lhcb5 proteins are depicted using the projection maps of monomeric LHCII components (133).

central protrusion in the side view (Figure 5*c*). The model implies that the 33-kDa subunit:PSII core monomer stoichiometry is 1:1. Some reports indicate the presence of two copies of the 33-kDa subunit per reaction center (72, 135, 136). However, the dimensions of the 33-kDa subunit protrusions shown in Figure 5 are consistent with single copies of the protein monomer (64).

Localization of the 23-kDa Extrinsic Subunits

When isolated in the presence of glycine betaine, PSII-LHCII supercomplexes additionally bind the 23-kDa subunit (EJ Boekema, J Nield, B Hankamer & J Barber, unpublished data). Preliminary difference mapping experiments suggested that the two lumenal protrusions in the side view projection map, located on either side of the 33-kDa components (Figure 5*c*), each contain a 23-kDa subunit. Similarly, positions in the top views, also identified by difference mapping, are shown in Figures 5*a* and 5*b*. These proposed positions are consistent with analysis of crystalline PSII arrays containing the 23-kDa subunit (76). Freeze-etching studies of the lumenal surface of the grana regions of thylakoid membranes (ESs surfaces) also show four lumenal protrusions (112) that could correspond to the four densities shown in Models 1 and 2 (Figures 5*a* and 5*b;* see section "Heterogeneity of PSII In Vivo"). If the PSII complexes studied, before and after the removal of extrinsic proteins by Ford et al (39), are interpreted as dimers, the positions attributed to the extrinsic subunits would be consistent with models shown in Figure 5.

Organization of the Membrane-Embedded PSII Core Components

Topological information is available on the organization of the subunits within the PSII reaction center complex. In its isolated form, the PSII reaction center consists of the α and β subunits of cyt *b*559 and PsbI (17, 91, 134). Crosslinking studies have shown that the α and β subunits of cyt *b*559 are closely associated with the D1 and D2 proteins (14, 88), whereas the stromally exposed N-terminus of PsbI is suggested to be in close contact with the D2 protein (128).

Sequence homology between the D1 and D2 subunits and the L and M subunits of purple bacteria suggest that the D1/D2 and L/M heterodimers are likely to have similar dimensions (approximately 70 × 30 Å) in the membrane plane (29). Cryo-electron crystallography studies have shown that the monomeric PSII RC-CP47 complex (dark-gray region) has dimensions of 81 × 75 Å (90), indicating that the estimated PSII RC size is reasonable.

Isolated RC-CP47 complexes (D1-D2-cyt *b*559-CP47) have also been subjected to crosslinking experiments, and the results indicate that CP47 is more

closely associated with D2 than with the other reaction center components (88). It is for this reason that CP47 is placed close to the D2 protein in both subunit organization models (Figures 5*a* and 5*b*).

There are currently no crosslinking data that help to position CP43 with respect to the D1-D2-cyt *b*559-CP47 complex. Consequently, at least two models can be proposed. In the first, CP47 is positioned between the reaction center components and CP43 (Model 1, Figure 5*a*). In the second, the reaction center components are located between CP43 and CP47 (Model 2, Figure 5*b*). Recently, PSII core dimer crystals were labeled with Fab antibody fragments, specific to the C-termini of the D1 protein and cyt *b*559 (75). These studies suggested that the D1 and cyt *b559* subunits were located farthest from CP43 but within the dark-gray region as shown in Model 1 (Figure 5*a*). However, crosslinking results of Seidler (114) detected interactions between the 23-kDa subunit and cyt *b*559, favoring Model 2 depicted in Figure 5*b*. The positions of cyt *b*559 as shown in Models 1 and 2 might allow the formation of an α-cyt *b*559 homodimer in crosslinking experiments carried out using D1-D2-cyt *b*559-CP47 complexes, assuming these preparations contained dimeric complexes (88).

Crosslinking and other biochemical studies have shown that CP43 (63) and cyt *b*559 (124, 125) are also closely associated with the 33-kDa subunit. Both cyt *b*559 and PsbI are estimated to be within 11 Å of the 33-kDa extrinsic polypeptide (37). Model 2 (Figure 5*b*) is more consistent with this combined data because it is difficult to see how CP43 and cyt *b*559 could interact simultaneously with the 33-kDa subunit in Model 1 (Figure 5*a*). Perhaps the most compelling evidence for the relative positioning of CP43 and CP47 on either side of the D1/D2 subunits (Model 2) comes from the comparison with the reaction center structure of PSI (42). This complex is composed of a heterodimer of PsaA and PsaB proteins each having 11 transmembrane helices. In each case, 5 of these helices are similarly arranged to the 5 helices of the L and M subunits of the purple bacterial reaction center (and presumably with the D1 and D2 proteins). The remaining 6 helices in each PSI subunit are positioned farther from the pseudo twofold axis that relates the two subunits in the heterodimer. Furthermore, the two sets of peripheral helices show sequence homology with those of CP47 and CP43. By analogy, therefore, it would seem reasonable to place CP43 and CP47 on either side of the D1 and D2 proteins.

Recently 3-D maps obtained from dimeric RC-CP47-CP43 complexes showed that the binding region for the 33-kDa subunit protrudes into the lumen (E Morris, B Hankamer, D Zheleva & J Barber, unpublished data). The D1 and D2 proteins, the α and β subunits of cyt *b*559 and PsbI, are all very

hydrophobic proteins with small lumenally exposed loops. In contrast, the lumenal loops E of CP47 and CP43 are large (22, 41, 45), suggesting that they could form part of this extrinsic region. This conclusion agrees well with the finding that loop E of CP47 is in close contact with the 33-kDa extrinsic polypeptide (23, 24, 41, 50, 94, 102). However, this information does not provide a sufficiently clear distinction between Models 1 and 2. This is because in Model 1, the 33-kDa subunit is positioned directly above CP47, allowing direct contact with loop E of the latter. However, in Model 2, CP47 is adjacent rather than directly under the 33-kDa subunit, and it is quite conceivable that loop E could fold over the lumenal surface of the centrally located D1/D2 heterodimer and so come into contact with the 33-kDa subunit.

Localization of the Lhcb Proteins

Western blot analysis of isolated PSII-LHCII supercomplexes showed them to be enriched in Lhcb1, Lhcb2, Lhcb4 (CP29), and Lhcb5 (CP26), but depleted of Lhcb3 and Lhcb6 (CP24) (93). Crosslinking studies have shown that CP47 and CP43 are both in close contact with CP29 (Lhcb4) and that CP43 is also in close contact with CP26 (Lhcb5) (26, 104). By superimposing a high-resolution electron density map of the Lhcb1/Lhcb2 heterotrimer (133) upon the top-view projection maps shown in Figure 5*a* and 5*b*, the LHCII complex can be seen to fit snugly into the two tips of the PSII-LHCII supercomplex. Furthermore, because Lhcb4 and 5 are similar in mass and have strong sequence homology with the LHCII proteins, two monomeric electron density maps based on the data of Wang & Kühlbrandt (133) were positioned in the PSII-LHCII supercomplex (in both Models 1 and 2) between the PSII core and the LHCII heterotrimer. There appears to be insufficient space to fit any additional monomeric Lhcb proteins. This conclusion is in agreement with pigment analyses of the isolated PSII-LHCII supercomplex, which showed it to be associated with 156 Chla and 46 Chlb molecules (see Figure 2*d* and 51, 52, 93). It was suggested that Lhcb6 (CP24) might also be present in these isolated PSII-LHCII supercomplexes (21), but this was a precautionary conclusion based on the detection of low levels of the protein present in early and less pure preparations. This conclusion has been amended in the light of the Western blot data presented by Hankamer et al (52) and Nield et al (93). The positions of Lhcb4 and 5 between the LHCII trimer and the PSII core is in agreement not only with the available crosslinking data (26, 104) but with the hypothesis that Lhcb4, 5, and 6 are involved in the regulation of the rate of excitation energy transfer from the outer Lhcb (Lhcb1, 2, and 3) proteins to the reaction center via CP47 and CP43 (see 65). However, the depletion of Lhcb3 and 6 in these complexes with respect to granal membranes must be explained.

One explanation is that the isolated PSII-LHCII supercomplex characterized originates from the population of ESs particles equivalent to those observed as arrays in freeze-etching studies of grana regions, and that Lhcb3 and Lhcb6 are associated predominantly with the nonarrayed ESs particles in the grana (see section on "Heterogeneity of PSII In Vivo"). This hypothesis is consistent with the isolation of a Lhcb6-Lhcb4-LHCII supramolecular complex (18). It is also consistent with the finding that PSIIα complexes in the grana consist of more than one subpopulation differing in antenna size (4, 5). Furthermore, the large distances between the nonarrayed ESs particles means that they may have larger antenna systems than their arrayed counterparts and could additionally bind Lhcb3 and Lhcb6 (see section on "Heterogeneity of PSII In Vivo").

The low-resolution subunit organizations presented in Figure 5, though incomplete, give two models that it is hoped will aid more detailed determinations of subunit organization and PSII structure in the future.

CONCLUDING REMARKS

The PSII-LHCII supercomplex is in projection possibly one of the largest integral membrane protein complexes in nature. Despite its large size, this discrete unit has escaped attention until recently. One of the reasons may be its thickness, which is only 60 Å at the outer ends. In fact, only the central parts, which are 90 Å in height, substantially protrude from the membrane and contribute to the appearance of the approximately 200 × 200 Å "particles," already seen long ago by freeze-fracture/freeze-etching techniques. No doubt, the PSII-LHCII supercomplex will provide a further basis for structural work, although its stability after isolation will possibly prevent the growing of highly ordered crystals. It is, however, highly suited for further single particle analysis using cryoelectron microscopy to produce a more detailed 3-D map suitable for the insertion of high-resolution data. Such data will almost certainly be obtained by crystallography (2-D and 3-D) of PSII complexes with smaller numbers of subunits or of individual subunits. In this way, the complete structure of PSII at atomic resolution will be built. Whether the high-resolution data will be obtained from X-ray or electron crystallography is uncertain, but with the successful outcome of the LHCII structure, the electron microscopy approach has yielded the most information to date for PSII. The instability of this photosystem, particularly when illuminated, presents a major hurdle that is unique to this complex. The authors are confident, however, that this hurdle will be surmounted in the not-too-distant future and that PSII, like the other major complexes of the photosynthetic electron transport chain, will have its structure determined at atomic resolution.

ACKNOWLEDGMENTS

In particular, we thank Lyn Barber for all her hard work and care in preparing this review and Jon Nield for his help in the figure preparation. We are also very grateful to Alain Brisson, Ed Morris, Jon Nield, Peter Nixon, Jyoti Sharma, Alison Telfer, and Daniella Zheleva for their critical proofreading of sections of the review and their constructive comments on them.

Literature Cited

1. Adir N, Okamura MY, Feher G. 1992. Crystallization of the PSII-reaction center. See Ref. 88a, 2:195–98
2. Akabori K, Imaoka A, Toyoshima Y. 1984. The role of lipids and 17-kDa protein in enhancing the recovery of O_2 evolution in cholate-treated thylakoid membranes. *FEBS Lett.* 173:36–40
3. Albertsson PA. 1995. The structure and function of the chloroplast photosynthetic membrane: a model for the domain organization. *Photosynth. Res.* 46:141–49
4. Albertsson PA, Yu SG. 1988. Heterogeneity among photosystem II. Isolation of thylakoid membrane vesicles with different functional antennae size of photosystem II. *Biochim. Biophys. Acta* 936:215–21
5. Albertsson PA, Yu SG, Larsson UK. 1990. Heterogeneity in Photosystem II. Evidence from fluorescence and gel electrophoresis experiments. *Biochim. Biophys. Acta* 1016: 137–40
6. Allen JF, Feher G, Yeates TO, Komiya H, Rees DC. 1987. Structure of the reaction center from *Rhodobacter sphaeroides* R-26: the co-factors. *Proc. Natl. Acad. Sci. USA* 84:5730–34
7. Anderson JM, Goodchild DM, Boardman NK. 1973. Composition of the photosystems and chloroplast structure in extreme shade plants. *Biochim. Biophys. Acta* 325: 573–85
8. Anderson JM, Melis A. 1983. Localization of different photosystems in separate regions of chloroplast membranes. *Proc. Natl. Acad. Sci. USA* 80:745–49
9. Andersson B, Åkerlund HE. 1987. Proteins of the oxygen-evolving complex. In *Topics in Photosynthesis, The Light Reactions,* ed. J Barber, 8:379–420. Amsterdam: Elsevier
10. Andersson B, Anderson JM. 1980. Lateral heterogeneity in the distribution of chlorophyll-protein complexes of the thylakoid membranes of spinach chloroplasts. *Biochim. Biophys. Acta* 593:427–40
11. Armond PA, Arntzen CJ. 1977. Localization and characterization of PSII in grana and stroma lamellae. *Plant Physiol.* 59: 398–404
12. Armond PA, Staehelin LA, Arntzen CJ. 1977. Spatial relationship of photosystem I, Photosystem II and the light harvesting complex in chloroplast membranes. *J. Cell. Biol.* 73:400–18
13. Babcock GT. 1987. The photosynthetic oxygen-evolving process. In *Photosynthesis,* ed. J Amesz, 15:125–58. Amsterdam: Elsevier
14. Barbato R, Friso G, Ponticos M, Barber J. 1995. Characterization of the light-induced cross-linking of the α-subunit of cytochrome b559 and the D1 protein in isolated Photosystem II reaction centers. *J. Biol. Chem.* 270:24032–37
15. Barber J. 1982. Influence of surface charges on thylakoid structure and function. *Annu. Rev. Plant Physiol.* 33:261–95
16. Barber J. 1987. Photosynthetic reaction centres: a common link. *Trends Biochem. Sci.* 12:323–26

16a. Barber J, ed. 1992. *The Photosystems: Structure, Function and Molecular Biology.* Amsterdam: Elsevier

17. Barber J, Chapman DJ, Telfer A. 1987. Characterisation of a photosystem II reaction centre isolated from chloroplasts of *Pisum sativum. FEBS Lett.* 220:67–73
18. Bassi R, Dainese P. 1992. A supramolecular light harvesting complex from chloroplast photosystem-II membranes. *Eur. J. Biochem.* 204:317–26
19. Bassi R, Ghiretti Magaldi A, Tognon G, Giacometti GM, Miller KR. 1989. Two-dimensional crystals of the Photosystem II

reaction center complex from higher plants. *Eur. J. Cell Biol.* 50:84–93
20. Bassi R, Pineau B, Dainese P, Marquardt J. 1993. Carotenoid-binding proteins of photosystem-II. *Eur. J. Biochem.* 212:297–303
21. Boekema EJ, Hankamer B, Bald D, Kruip J, Nield J, et al. 1995. Supramolecular structure of the photosystem II complex from green plants and cyanobacteria. *Proc. Natl. Acad. Sci. USA* 92:175–79
22. Bricker TM. 1990. The structure and function of CPa-1 and CPa-2 in photosystem II. *Photosynth. Res.* 24:1–13
23. Bricker TM, Frankel LK. 1987. Use of monoclonal antibody in structural investigations of the 49 kDa polypeptide of photosystem II. *Arch. Biochem. Biophys.* 256: 295–301
24. Bricker TM, Odom WR, Queirolo CB. 1988. Close association of the 33-kDa extrinsic protein with the apoprotein of CPA1 in photosystem-II. *FEBS Lett* 231:111–17
25. Britt RD. 1996. Oxygen evolution. See Ref. 95a, pp. 137–59
26. Dainese P, Santini C, Ghiretti-Magaldi A, Marquardt J, Tidu V, et al. 1992. The organisation of pigment proteins within photosystem II. See Ref. 88a, 2:13–20
27. Deisenhofer J, Epp O, Miki K, Huber R, Michel H. 1984. X-ray structure analysis of a membrane protein: electron density map at 3Å resolution and a model of the photosynthetic reaction center from *Rhodopseudomonas viridis*. *J. Mol. Biol.* 180: 385–98
28. Deisenhofer J, Epp O, Miki K, Huber R, Michel H. 1985. Structure of the protein subunits in the photosynthetic reaction centre of *Rhodopseudomonas viridis* at 3Å resolution. *Nature* 318:618–24
29. Deisenhofer J, Michel H. 1989. The photosynthetic reaction center from the purple bacterium *Rhodopseudomonas viridis*. *EMBO J.* 8:2149–70
30. Dekker JP, Boekema EJ, Witt HT, Rögner M. 1988. Refined purification and further characterization of oxygen-evolving and Tris-treated photosystem-II particles from the thermophilic cyanobacterium *Synechococcus* sp. *Biochim. Biophys. Acta* 936: 307–18
31. Dekker JP, Bowlby NR, Yocum CF, Boekema EJ. 1990. Characterization by electron microscopy of isolated particles and two-dimensional crystals of the CP47-D1-D2-cytochrome b–559 complex of Photosystem II. *Biochemistry* 29:3220–25
32. Demmig-Adams B. 1990. Carotenoids and photoprotection in plants: a role for the xanthophyll zeaxanthin. *Biochim. Biophys. Acta* 1020:1–24
33. de Vitry C, Olive J, Drapier D, Recouvreur M, Wollman FA. 1989. Post-translational events leading to the assembly of photosystem II protein complex: a study using photosynthesis mutants from *Chlamydomonas reinhardtii*. *J. Cell Biol.* 109:991–1006
34. Diner BA, Petrouleas V, Wendoloski JJ. 1991. The iron-quinone electron-acceptor complex of photosystem II. *Physiol. Plant.* 81:423–36
35. Dostatni R, Meyer HE, Oettmeier W. 1988. Mapping of two tyrosine residues involved in the quinone (Q_B) binding site of the D1 reaction center polypeptide of photosystem II. *FEBS Lett.* 239:207–10
36. Durrant JR, Klug DR, Kwa SLS, van Grondell R, Porter G, Dekker JP. 1995. A multimer model for P680, the primary electron donor of PSII. *Proc. Natl. Acad. Sci. USA* 92:4798–802
37. Enami I, Ohta S, Mitsuhashi S, Takahashi S, Ikeuchi M, Katoh S. 1992. Evidence from crosslinking for a close association of the extrinsic 33 kDa protein with the 9.4 kDa subunit of cytochrome b559 and the 4.8 kDa product of the psbI gene in oxygen evolving photosystem II complexes from spinach. *Plant Cell Physiol.* 33:291–97
38. Erickson JM, Rochaix JD. 1992. The molecular biology of photosystem II. See Ref. 16a, 2:101–77
39. Ford RC, Rosenberg MF, Shepherd FH, McPhie P, Holzenburg A. 1995. Photosystem II 3-D structure and the role of the extrinsic subunits in photosynthetic oxygen evolution. *Micron* 26:133–40
40. Fotinou C, Kokkinidis M, Fritzsch G, Haase W, Michel H, Ghanotakis DF. 1993. Characterization of a photosystem-II core and its 3-D crystals. *Photosynth. Res.* 37: 41–48
41. Frankel LK, Bricker TM. 1992. Interaction of CPa-1 with the manganese-stabilizing protein of photosystem II: identification of domains on CPa-1 which are shielded from N-hydroxysuccinimide biotinylation by the manganese-stabilizing protein. *Biochemistry* 31:11059–64
42. Fromme P, Witt HT, Schubert WD, Klukas O, Saenger W, Krauss N. 1996. Structure of photosystem-I at 4.5-Å resolution: a short review including evolutionary aspects. *Biochim. Biophys. Acta* 1275:76–83
43. Ghanotakis DF, Topper JN, Babcock GT, Yocum CF. 1984. Water-soluble 17-kDa and 23-kDa polypeptides restore oxygen evolution activity by creating a high-affin-

ity binding-site for Ca^{-2} and on the oxidizing side of photosystem-II. *FEBS Lett.* 170: 169–73
44. Ghanotakis DF, Yocum CF. 1985. Polypeptides of photosystem II and their role in oxygen evolution. *Photosynth. Res.* 7: 97–114
45. Gleiter HM, Haag E, Shen JR, Eaton-Rye JJ, Inoue Y, et al. 1994. Functional characterization of mutant strains of the cyanobacterium *Synechocystis* sp. PCC 6803 lacking short domains within the large, lumen-exposed loop of the chlorophyll protein CP47 in photosystem II. *Biochemistry* 33:12063–71
46. Green BR, Durnford DG. 1996. The chlorophyll-carotenoid proteins of oxygenic photosynthesis. *Annu. Rev. Plant Physiol. Plant Mol. Biol.* 47:685–714
47. Green BR, Durnford DG, Aebersold R, Pichersky E. 1992. Evaluation of structure and function in the Chl a/b and Chl a/c antenna protein family. See Ref. 88a, 1: 195–202
48. Green BR, Pichersky E. 1994. Hypothesis for the evolution of three-helix Chl a/b and Chl a/c light-harvesting antenna proteins from two-helix and four-helix ancestors. *Photosynth. Res.* 39:149–62
49. Green BR, Pichersky E, Kloppstech K. 1991. Chlorophyll a/b binding proteins: an extended family. *Trends Biochem. Sci.* 16: 181–86
50. Haag E, Eaton-Rye JJ, Renger G, Vermaas WFJ. 1993. Functionally important domains of the large hydrophilic loop of CP47 as probed by oligonucleotide directed mutagenesis in *Synechocystis* sp. PCC6803. *Biochemistry* 32:4444–54
51. Hankamer B, Morris E, Zheleva D, Barber J. 1995. Biochemical characterisation and structural analysis of monomeric and dimeric photosystem II core preparations. See Ref. 76a, 3:365–68
52. Hankamer B, Nield J, Zheleva D, Boekema E, Jansson S, Barber J. 1996. Isolation and biochemical characterisation of monomeric and dimeric PSII complexes from spinach and their relevance to the organisation of photosystem II *in vivo*. *Eur. J. Biochem.* 243:422–29
53. Hansson Ö, Wydrzynski T. 1990. Current perceptions of photosystem II. *Photosynth. Res.* 23:131–62
54. Henderson R. 1995. The potential and limitations of neutrons, electrons and X-rays for atomic resolution microscopy of unstained biological molecules. *Q. Rev. Biophys.* 28:171–93
55. Henriques F, Park RB. 1975. Further chemical and morphological characterization of chloroplast membranes from a chlorophyll b-less mutant of *Hordeum vulgare*. *Plant Cell Physiol.* 55:763–67
56. Henriques F, Park RB. 1976. Development of the photosynthetic unit in lettuce. *Proc. Natl. Acad. Sci. USA* 73:4560–64
57. Henrysson T, Sundby C. 1990. Characterisation of photosystem II in stroma thylakoid membranes. *Photosynth. Res.* 25: 107–17
58. Hiratsuka J, Shimada H, Whittie R, Ishibashi T, Sakamoto M, et al. 1989. The complete sequence of the rice (*Oryza sativa*) chloroplast genome: intermolecular recombination between distinct transferRNA genes accounts for a major plastid DNA inversion during the evolution of the cereals. *Mol. Gen. Genet.* 217:185–94
59. Hirschberg J, McIntosh L. 1983. Molecular basis of herbicide resistance in *Amaranthus hybridus*. *Science* 222:1346–49
60. Hoganson CW, Lydakis-Simantiris N, Tang XS, Tommos C, Warncke K, et al. 1995. A hydrogen-atom abstraction model for the function of Y_Z in photosynthetic oxygen-evolution. *Photosynth. Res.* 46: 177–84
61. Holzenburg A, Bewly MC, Wilson FH, Nicholson WV, Ford RC. 1993. Three-dimensional structure of photosystem II. *Nature* 363:470–72
62. Horton P, Ruban AV, Walters RG. 1996. Regulation of light-harvesting in green plants. *Annu. Rev. Plant Physiol. Plant Mol. Biol.* 47:655–84
63. Isogai Y, Yamamoto Y, Nishimura M. 1985. Association of the 33-kDa polypeptide with the 43-kDa component in photosystem II particles. *FEBS Lett.* 187:240–44
64. Jansen T, Rother C, Steppuhn J, Reinke H, Beyreuther K, et al. 1987. Nucleotide sequence of cDNA clones encoding the complete 23-kDa and 16-kDa precursor proteins associated with the photosynthetic oxygen evolving complex from spinach. *FEBS Lett.* 216:234–40
65. Jansson S. 1994. The light-harvesting chlorophyll a/b-binding proteins. *Biochim. Biophys. Acta* 1184:1–19
66. Joliot P, Barbier IG, Chabaud R. 1969. Un nouveau modúle des centres photochimique du systeme II. *Photochem. Photobiol.* 10:309–29
67. Keck RW, Dilley RA, Allen CF, Biggs S. 1970. Chloroplast composition and structural differences in a soybean mutant. *Plant Physiol.* 46:692–98
68. Kok B, Forbush B, McGloin M. 1970. Cooperation of charges in photosynthetic evo-

lution. I. A linear four step mechanism. *Photochem. Photobiol.* 11:457–75
69. Kühlbrandt W, Wang DN, Fujiyoshi Y. 1994. Atomic model of plant light-harvesting complex by electron crystallography. *Nature* 367:614–21
70. Lam E, Baltimore B, Ortiz W, Chollar S, Melis A, Malkin R. 1983. Characterization of a resolved oxygen-evolving photosystem-II preparation from spinach thylakoids. *Biochim. Biophys. Acta* 724:201–11
71. Lancaster CRD, Michel H, Honig B, Gunner MR. 1996. Calculated coupling of electron and proton-transfer in the photosynthetic reaction-center of *Rhodopseudomonas viridis*. *Biophys. J.* 70:2469–92
72. Leuschner C, Bricker TM. 1996. Interaction of the 33 kDa protein with photosystem II: rebinding of the 33 kDa extrinsic protein to photosystem II membranes which contain four, two, zero manganese per photosystem II reaction center. *Biochemistry* 35: 4551–57
73. Lorkovic ZJ, Schröder WP, Pakrasi HB, Irrgang KD, Herrmann RG, Oelmuller R. 1995. Molecular characterization of PsbW, a nuclear-encoded component of the photosystem-II reaction-center complex in spinach. *Proc. Natl. Acad. Sci. USA* 92: 8930–34
74. Lyon MK, Marr KM, Furcinitti PS. 1993. Formation and characterization of two-dimensional crystals of photosystem II. *J. Struct. Biol.* 110:133–40
75. Marr KM, Mastronarde DM, Lyon MK. 1996. Two-dimensional crystals of photosystem II: biochemical characterization, cryoelectron microscopy and localization of the D1 and cytochrome b559 polypeptides. *J. Cell Biol.* 132:823–33
76. Marr KM, McFeeters RL, Lyon MK. 1996. Isolation and structural analysis of two-dimensional crystals of photosystem II from *H. vulgare viridis* zb63. *J. Struct. Biol.* 117: 86–98
76a. Mathis P, ed. 1995. *Photosynthesis: From Light to Biosphere*. The Netherlands: Kluwer
77. McDermott G, Prince SM, Freer AA, Hawthornthwaite-Lawless AM, Papiz MZ, et al. 1995. Crystal structure of an integral membrane light-harvesting complex from photosynthetic bacteria. *Nature* 374:517–21
78. McPherson PH, Schönfeld M, Paddock ML, Okamura MY, Feher G. 1994. Protonation and free energy changes associated with formation of Q_BH_2 in native and Glu-L212→Gln mutant reaction centers from *Rhodobacter sphaeroides*. *Biochemistry* 33:1181–93
79. Michel H, Deisenhofer J. 1988. Relevance of the photosynthetic reaction center from purple bacteria to the structure of photosystem II. *Biochemistry* 27:1–7
80. Miller KR. 1981. Freeze-etching studies of photosynthetic membranes. In *Electron Microscopy in Biology*, ed. JD Griffith, 1:1–30. New York: Wiley-Interscience
81. Miller KR, Cushman RA. 1978. A chloroplast membrane lacking photosystem II. *Biochim. Biophys. Acta* 546:481–99
82. Miller KR, Jacob JS. 1991. Surface structure of the photosystem II complex. In *Proc. EMSA Meet., 49th*, ed. GW Bailey. San Francisco: San Francisco Press
83. Miller KR, Miller GJ, McIntyre KR. 1976. The light-harvesting chlorophyll-protein complex of photosystem II. *J. Cell Biol.* 71:624–38
84. Miller KR, Miller GJ, McIntyre KR. 1977. Organization of the photosynthetic membrane in maize mesophyll and bundle sheath chloroplasts. *Biochim. Biophys. Acta* 459:145–56
85. Miller KR, Staehelin LA. 1976. Analysis of the thylakoid outer surface. Coupling factor is limited to unstacked membrane regions. *J. Cell Biol.* 68:30–47
86. Miyao M, Murata N. 1984. Role of the 33kDa polypeptide in preserving Mn in the photosynthetic oxygen-evolving system and its replacement by chloride ions. *FEBS Lett.* 170:350–54
87. Miyao M, Murata N. 1984. Calcium ions can be substituted for the 24-kDa polypeptide in photosynthetic oxygen evolution. *FEBS Lett.* 168:118–20
88. Moskalenko AA, Barbato R, Giacometti GM. 1992. Investigation of the neighbour relationships between PSII polypeptides in the two types of isolated reaction centres (D1/D2/cytb559 and CP47/D1/D2/cytb559 complexes). *FEBS Lett.* 314:271–74
88a. Murata N, ed. 1992. *Research in Photosynthesis*. Dordrecht: Kluwer
89. Murata N, Miyao M. 1985. Extrinsic membrane proteins in the photosynthetic oxygen-evolving complex. *Trends Biochem. Sci.* 10:122–24
90. Nakazato K, Toyoshima C, Enami I, Inoue Y. 1996. Two-dimensional crystallization and cryo-electron microscopy of photosystem II. *J. Mol. Biol.* 257:225–32
91. Nanba O, Satoh K. 1987. Isolation of a photosystem II reaction center consisting of D-1 and D-2 polypeptides and cytochrome b-559. *Proc. Natl. Acad. Sci. USA* 84:109–12
92. Nicholson WV, Shepherd FH, Rosenberg MF, Ford RC, Holzenburg A. 1996. Struc-

ture of photosystem II in spinach thylakoid membranes: comparison of detergent-solubilized and native complexes by electron microscopy. *Biochem. J.* 315:543–47

93. Nield J, Hankamer B, Zheleva D, Hodges ML, Boekema EJ, Barber J. 1995. Biochemical characterisation of PSII-LHCII complexes associated with and lacking the 33 kDa subunit. See Ref. 76a, 3:361–64
94. Odom WR, Bricker TM. 1992. Interaction of CPa-1 with the Manganese-Stabilizing protein of photosystem II: identification of domains cross-linked by 1-ethyl-3-[3-(dimethylamino)-propyl] carbimide. *Biochemistry* 31:5616–20
95. Olive J, Vallon O. 1991. Structural organization of the thylakoid membrane: freeze-fracture and immuno-cytochemical analysis. *J. Electron Microsc. Tech.* 18:360–74

95a. Ort DR, Yocum CF, eds. 1996. *Oxygenic Photosynthesis: The Light Reactions*. Dordrecht: Kluwer

96. Paddock ML, Feher G, Okamura MY. 1995. Pathway of proton transfer in bacterial reaction centers: further investigations on the role of Ser-L223 studied by site-directed mutagenesis. *Biochemistry* 34: 15742–50
97. Paulsen H. 1995. Chlorophyll a/b binding proteins. *Photochem. Photobiol.* 62:367–82
98. Pecoraro VL, Gelasco A, Baldwin M. 1995. Modeling the chemistry and properties of multinuclear manganese enzymes. In *Bioinorganic Chemistry,* ed. DP Kessissoglu, pp. 287–98. Dordrecht: Kluwer
99. Peter GF, Thornber JP. 1991. Biochemical evidence that the higher plant photosystem II core complex is organized as a dimer. *Plant Cell Physiol.* 32:1237–50
100. Peter GF, Thornber JP. 1991. Biochemical composition and organisation of higher plant photosystem II light harvesting pigment-proteins. *J. Biol. Chem.* 266: 16745–54
101. Popov VI, Tageeva SV, Kaurov BS, Gavrilov AG, Rubin AB, Rubin LB. 1977. Effect of ruby laser illumination on the ultrastructure of pea chloroplast membranes. *Photosynthetica* 11:76–80
102. Putnam-Evans C, Bricker TM. 1992. Site-directed mutagenesis of the CP–1 protein of photosystem II: alteration of the basic pair 384, 385R to 484, 385G leads to a defect association with the O_2 evolving complex. *Biochemistry* 31:11482–88
103. Renger G, Rutherford AW, Völker M. 1985. Evidence for resistance of the micro environment of the primary plastoquinone acceptor ($Q_A^-Fe^{2+}$) to mild trypsination in PSII particles. *FEBS Lett.* 185:243–47
104. Rigoni F, Barbato R, Friso G, Giacometti GM. 1992. Evidence for direct interaction between the chlorophyll-proteins CP29 and CP47 in Photosystem II. *Biochem. Biophys. Res. Commun.* 184:1094–100
105. Rochaix JD, Erickson J. 1988. Function and assembly of photosystem II-genetic and molecular analysis. *Trends Biochem. Sci.* 13:56–59
106. Rögner M, Boekema EJ, Barber J. 1996. How does photosystem 2 split water? The structural basis of efficient energy conversion. *Trends Biochem. Sci.* 21:44–49
107. Ruffle SV, Donelly D, Blundell TL, Nugent JHA. 1992. A three dimensional model of the photosystem II reaction centre of *Pisum sativum*. *Photosynth. Res.* 34:287–300
108. Rutherford AW, Zimmermann JL, Boussac A. 1992. Oxygen evolution. See Ref. 16a, 2:179–229
109. Santini C, Tidu V, Tognon G, Ghiretti Magaldi A, Bassi R. 1994. Three-dimensional structure of higher plant photosystem II reaction centre and evidence for its dimeric organization. *Eur. J. Biochem.* 221:307–15
110. Satoh K. 1993. Isolation and properties of the photosytem II reaction center. In *The Photosynthetic Reaction Center,* ed. J Deisenhofer, JR Norris, pp. 289–318. New York: Academic
111. Satoh K. 1996. Introduction to the Photosystem II reaction center: isolation and biochemical and biophysical characterisation. See Ref. 95a, pp. 193–207
112. Seibert M, DeWit M, Staehelin LA. 1987. Structural localization of the O_2-evolving apparatus to multimeric (tetrameric) particles on the lumenal surface of freeze-etched photosynthetic membranes. *J. Cell Biol.* 105:2257–65
113. Shinkarev VP, Takahashi E, Wraight CA. 1993. Flash-induced electric potential generation in wild type and L212EQ mutant chromatophores *of Rhodobacter sphaeroides:* Q_BH_2 is not released from L212EQ mutant reaction centers. *Biochim. Biophys. Acta* 1142:214–16
114. Seidler A, 1996. The extrinsic polypeptides of photosystem II. *Biochim. Biophys. Acta* 1277:35–60
115. Simpson DJ. 1978. Freeze-fracture studies on barley plastid membranes II. Wild-type chloroplast. *Carlsberg Res. Commun.* 43: 365–89
116. Simpson DJ. 1979. Freeze-fracture studies on barley plastid membranes. III. Location of the light harvesting chlorophyll-protein. *Carlsberg Res. Commun.* 44:305–36

117. Simpson DJ. 1982. Freeze-fracture studies on barley plastid membranes *V. viridis*-n34, a photosystem I mutant. *Carlsberg Res. Commun.* 47:215–25
118. Simpson DJ, Lindberg Møller B, Høyer-Hansen G. 1978. Freeze-fracture structure and polypeptide composition of thylakoids of wild type and mutant barley plastids. In *Chloroplast Development,* ed. G Akoyunoglou, pp. 507–12. Amsterdam: Elsevier/North-Holland Biomed.
119. Staehelin LA. 1975. Chloroplast membrane structure. Intramembranous particles of different sizes make contact in stacked membrane regions. *Biochim. Biophys. Acta* 408:1–11
120. Staehelin LA. 1976. Reversible particle movements associated with unstacking and restacking of chloroplast membranes *in vitro*. *J. Cell Biol.* 71:136–58
121. Staehelin LA. 1986. Chloroplast structure and supramolecular organization of photosynthetic membranes. In *Photosynthesis III, Photosynthetic Membranes and Light Harvesting Systems,* ed. LA Staehelin, CJ Arntzen, pp. 1–84. Berlin: Springer
122. Staehelin LA, Armond PA, Miller KR. 1976. Chloroplast membrane organisation at the supramolecular level and its functional implications. *Brookhaven Symp. Biol.* 28:278–315
123. Svensson B, Vass I, Cedergren E, Styring S. 1990. Structure of donor side components in photosystem II predicted by computer modelling. *EMBO J.* 9:2051–59
124. Tae GS, Black MT, Cramer WA, Vallon O, Bogorad L. 1988. Thylakoid membrane protein topography: Transmembrane orientation of the chloroplast cytochrome b559 *psbE* gene product. *Biochemistry* 27: 9075–80
125. Takahashi Y, Asada K. 1991. Determination of the molecular size of the binding site for the manganese-stabilizing 33 kDa protein in photosystem II membranes. *Biochim. Biophys. Acta* 1059:36–64
126. Tang XS, Fushimi K, Satoh K. 1990. D1-D2 complex of the photosystem II reaction center from spinach: isolation and partial characterization. *FEBS Lett.* 273:257–60
127. Tommos C, Tang XS, Warncke K, Hoganson CW, Styring S, et al. 1995. Spin-density distribution, conformation and hydrogen bonding of the redox-active tyrosine Y_Z in PSII from multiple electron magnetic-resonance spectroscopies: implications for photosynthetic oxygen evolution. *J. Am. Chem. Soc.* 117:10325–35
128. Tomo T, Enami I, Satoh K. 1993. Orientation and nearest neighbor analysis of psbI gene product in the photosystem II reaction center complex using bifunctional cross-linkers. *FEBS Lett.* 323:15–18
129. Trebst A. 1986. The topology of plastoquinone and herbicide binding peptides of photosystem II in the thylakoid membrane. *Z. Naturforsch. Teil C* 41:240–45
130. Tsiotis G, Walz T, Spyridaky A, Lustig A, Engel E, Ghanotakis D. 1996. Tubular crystals of a photosystem II core complex. *J. Mol. Biol.* 259:241–48
131. Tsvetkova NM, Apostolova EL, Brain APR, Williams WP, Quinn PJ. 1995. Factors influencing PSII particle array formation in *Arabidopsis thaliana* chloroplasts and the relationship of such arrays to the thermostability of PSII. *Biochim. Biophys. Acta* 1228:201–10
132. van Mieghem FJE, Satoh K, Rutherford AW. 1991. A chlorophyll tilted 30° relative to the membrane in the PSII reaction centre. *Biochim. Biophys. Acta* 1058:375–78
133. Wang DN, Kühlbrandt W. 1991. High-resolution electron crystallography of light-harvesting chlorophyll-a/b-protein complex in 3 different media. *J. Mol. Biol.* 217:691–99
134. Webber AN, Packman LC, Chapman DJ, Barber J, Gray JC. 1989. A 5th chloroplast-encoded polypeptide is present in the photosystem II reaction center complex. *FEBS Lett.* 242:259–62
135. Xu Q, Bricker TM. 1992. Structural organization of proteins on the oxidizing side of Photosystem II. *J. Biol. Chem.* 267: 25816–21
136. Yamamoto Y, Tabata K, Isogai Y, Nishimura M, Okayama S, et al. 1984. Quantitative analysis of membrane components in a highly active O_2-evolving photosystem II preparation from spinach chloroplasts. *Biochim. Biophys. Acta* 767: 493–500
137. Yu C-A, Xia J-Z, Kachurin AM, Yu L, Xia D, et al. 1996. Crystallization of preliminary structure of beef heart mitochondrial cytochrome-bc1 complex. *Biochim. Biophys. Acta* 1275:47–53